

Investigating the Change of Discharge Behavior of Gas and Liquid by Means of Analytical and Numerical Approaches

**Laura Cordes, Lisa Hühn,
Corina Schwitzke, Hans-Jörg Bauer**
Institute of Thermal Turbomachinery (KIT)
laura.cordes@kit.edu
Karlsruhe, Germany

ABSTRACT

The presented work discusses the differences between a gaseous and liquid flow through an orifice. The goal is to use the available data on air flow through orifices of different geometries and for a wide range of boundary conditions and apply it to the flow of a liquid.

In order to do so, the equations for the calculation of the discharge coefficient and the ideal velocity in the orifice are developed for an incompressible fluid and compared to the equations for a compressible fluid. The changes that occur by using this approach for the incompressible fluid, and by increasing the density up to 1000 times the density of air are evaluated analytically.

The effect of incompressibility and density increase on the real flow behavior is investigated numerically. This is done by changing the fluids properties independently allowing resulting effects to be evaluated separately. Results show that while a density increase causes a significant drop of the discharge coefficient, at the same time the incidence angle rises. Correlating the discharge coefficient with the incidence angle represents the influence of density and incompressibility very well if the boundary conditions are kept constant.

INTRODUCTION

The demand for further increase of jet engine efficiency has led to the introduction of gearboxes between low pressure spool and fan shaft. Cooling and lubrication of the gearbox becomes crucial. Thus it needs to be sufficiently supplied with oil. Therefore, the oil has to be transported from a static tank into the rotating gear system with minimum pressure losses. The challenge of designing an optimized discharge system shows similarities to the secondary air system. For these applications the discharge behaviour of gases such as air has been investigated by many researchers intensively in the past decades. The influence of different orifice geometries and boundary conditions, such as length-to-diameter ratio and

chamfered edges, or pressure ratios and flow inclination, respectively, have been studied.

Most investigations focus on the determination of flow related losses. The following section will provide an overview of relevant literature. Some of the work was carried out by means of combination of CFD simulations and experiments to understand the physical mechanisms affecting the discharge behavior.

McGreehan et al. [9] presented a variety of early work on rotating orifices. They postulated that the rotation of an orifice can be regarded as a stationary orifice with a flow approaching at an angle.

Zimmermann et al. [13] were the first to evaluate the discharge coefficient in a relative frame of reference. With this transformation, it is possible to compare existing experimental data of previous work. The focus of the work performed by Alexiou et al. [1, 1] is the effect of rotation on the flow behavior in the orifice. They found that the discharge coefficient decreases with increasing rotational speed. An enlarged separation in the orifice is responsible for this effect.

To reduce the flow-related losses Dittmann et al. varied the geometrical parameters of the orifices [2] and investigated the effect of a pre-swirled flow [3]. The inlet geometry of the orifice significantly influences the separation regions in the orifices. With larger length-to-diameter ratios jet reattachment can occur inside the orifice.

Idris et al. summarized the influence of different parameters on the flow behaviour [5]. Their research is based on the database available in existing literature as well as their own numerical and experimental data. They found that correlating the discharge behaviour with the angle of inclination i enables the comparison of results for different boundary conditions, orifice geometries and inclination angles [4, 6]. Inclining the orifices with the angle β_0 or imposing a pre-swirl onto the incident flow can improve the discharge behaviour, by reducing the angle of inclination. Sousek

produced numerous experimental and numerical data for different configurations including pre-swirled flow [11].

Wilk et al. [12] carried out one of the first investigations on liquid flow passing through rotating axial orifices. They found a good correlation between the discharge coefficient and the Strouhal number. A result of their research was that due to the different fluid behaviour of gas and liquid and the different mathematical treatment it is not possible to compare the discharge coefficient of air and liquid flow directly.

DATA ANALYSIS

The flow through an orifice is usually characterized by the discharge coefficient c_d , which is the ratio of the actual mass flow rate and the ideal mass flow rate through an orifice.

$$c_d = \frac{\dot{m}_{re}}{\dot{m}_{id}} \quad (1)$$

The ideal mass flow rate is

$$\dot{m}_{id} = \rho A c_{id}, \quad (2)$$

with the ideal velocity in the orifice c_{id} . Considering a gas flowing through the orifice driven by a pressure ratio Π and assuming an isentropic expansion it yields

$$c_{id} = \sqrt{\frac{2\gamma}{\gamma-1} RT_{1s} \left(1 - \left(\frac{p_{2s}}{p_{1s}} \right)^{\frac{\gamma-1}{\gamma}} \right)} \quad (3)$$

for the case that the kinetic energy upstream of the orifice is negligible. For rotating orifices Zimmerman et al. [13] proposed to determine the ideal velocity in the system relative to the orifice. Consequently, the static properties upstream of the orifice are replaced by the total properties in the relative system.

$$c_{id,rel} = \sqrt{\frac{2\kappa}{\gamma-1} RT_{1t,rel} \left(1 - \left(\frac{p_{2s}}{p_{1t,rel}} \right)^{\frac{\gamma-1}{\gamma}} \right)} \quad (4)$$

This has the advantage that the work input from the rotor is taken into account for the calculation of the ideal mass flow rate. Otherwise, discharge coefficients larger than one may occur.

Equations 3 and 4 are not applicable for liquids. In this case Wilk [12] used Torricelli's formula to calculate the ideal velocity in the orifice.

$$c_{id} = \sqrt{\frac{2 \Delta p}{\rho}} \quad (5)$$

Applying the moving reference frame equation 5 becomes

$$c_{id,rel} = \sqrt{\frac{2}{\rho} (p_{1t,rel} - p_{2s})}, \quad (6)$$

with $p_{1t,rel}$ representing the total pressure defined in the moving reference frame.

The real mass flow rate needs to be determined experimentally or numerically. It strongly depends on the phenomena occurring in the flow, such as separation or reattachment, and therefore on the fluid properties.

The discharge coefficient is usually correlated with a dimensionless quantity. To capture the influence of the inflow conditions and of the rotating system the ratio of the velocity of the orifices in the absolute reference frame U to the ideal velocity of the flow in the orifice c_{id} may be used. Using the ideal velocity in the relative system is beneficial here as well, because the ratio $U/c_{id,rel}$ does not exceed infinity [13]. Dittmann [3] used the tangential velocity of the approaching flow in the relative system instead of U to describe the flow's pre-swirl. Idris [4] interpreted these velocities in a velocity triangle and derived the relative inlet velocity angle β_1 . Later they expanded their approach for cases, in which the incoming flow has a pre-swirl concluding that the angle of attack i between β_1 and the axis of the orifice is an appropriate measure for correlation. In this case the orifice velocity needs to be replaced with the inlet flow velocity relative to the orifice $v_{1,rel}$. In Figure 1 the angular relations between an inclined orifice and the flow velocity in the relative reference frame $v_{1,rel}$ is depicted. The inclination angle of the orifice is β_0 . The relative velocity W results from the ideal velocity through the orifice $c_{id,rel}$ and the inlet flow velocity relative to the orifice $v_{1,rel}$. The relative inlet velocity angle β_1 is between W and $c_{id,rel}$. The difference between β_1 and β_0 yields the incidence angle i . As often used in turbomachinery, angles and velocity components in the direction of rotation are positive and vice versa [7]. Therefore, all angles depicted in Figure 1 are negative.

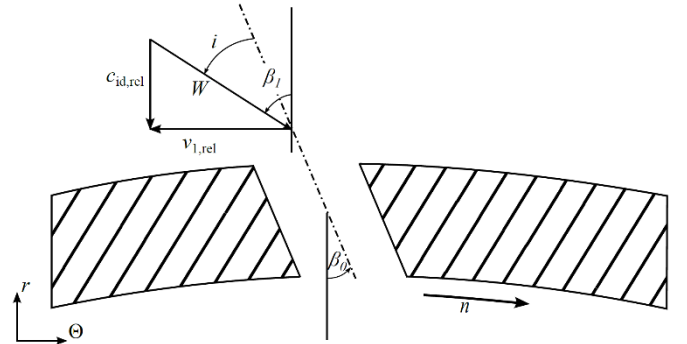


Figure 1: Angular relations for an orifice, inclined by the angle β_0 and rotating with the velocity U

All of the aforementioned sources are based on air as their flow medium. The only available source in literature describing a liquid flow, namely water, is by Wilk [12]. He performed a dimensional analysis and found a correlation of the discharge coefficient

$$c_d = 0.183 \ln \left(\frac{3}{S} + 1 \right), \quad (7)$$

depending on the Strouhal number

$$S = \frac{u}{2\pi c_{re}}. \quad (8)$$

The main difference to the correlations by Idris and Dittmann is that for equation 8 the actual velocity c_{re} through the orifice is used instead of the ideal velocity c_{id} . Wilk states in his discussion, that the results from an air flow are not transferrable to a liquid. He justifies this with the differences in the calculation of the discharge coefficient. Furthermore, Wilk names the fluid's internal forces as an important factor for the discharge behavior. According to his investigations this is the reason why he found very small discharge coefficients around 0.05.

NUMERICAL SET-UP

For the present study the real mass flow rate is determined by means of numerical simulations. This has the advantage that the fluid properties can be varied independently, creating fluids that do not exist in reality. This allows the quantification of the individual parameter's influence.

The three-dimensional simulations are based on the experimental set-up and numerical work from Sousek [11]. It was chosen because it is well described and sufficient experimental data is available [10] to validate the accuracy of the model for the present study. In Figure 2 the computational domain and the boundary conditions are shown. The domain consists of one 60° sector of the whole circumference. It has one velocity inlet and two pressure outlets. The static pressures applied to the pressure outlets are derived from two pressure ratios investigated by Sousek: $\Pi = 1.05$ and 1.3. They were chosen to include one case with very small compressibility effects, and one case where compressibility effects are expected. All shafts rotate with the rotational speed n and are conditioned with no-slip walls. The inlet velocity is defined in the rotating reference frame. For the reference case is set to $v_{ax,ref} = 34$ m/s. Multiple calculations with increasing densities up to 1000 times that of air, and otherwise constant boundary conditions were performed. For some cases the inlet velocity is changed to achieve a specific momentum. In Table 1 the applied parameters are given.

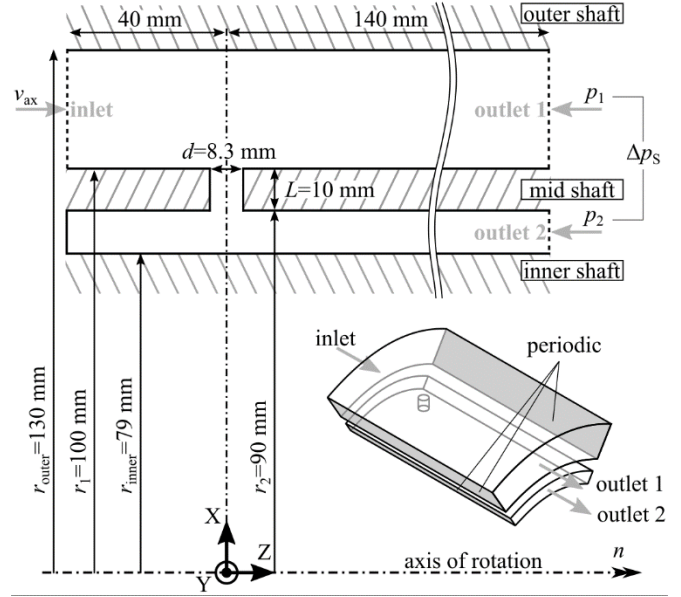


Figure 2: Computational domain

The mesh is defined in the moving reference frame and rotates with the shafts. It is block structured with an O-Grid in the orifice. Where y^+ is greater than one, enhanced wall treatment is used.

The results from the simulations are, for the cases with the density of air, in good agreement with the experimental data from Sousek [11], with a maximum deviation of 7 %. This allows the assumption of a validated numerical model.

Table 1: Parameters of the numerical set-up

v_{ax}	0.2 – 34 m/s
n	16,67 Hz (1000 rpm)
p_1	1 bar
Δp_s	$5 \cdot 10^3$ Pa ; $24 \cdot 10^3$ Pa ; $50 \cdot 10^3$ Pa
ρ	1.25 – 1250 kg/m ³
Turbulence Model	k- ϵ
Wall treatment	Two-Layer model and enhanced wall treatment by Kader [8]
Solution Method	100 iterations steady (COUPLED) 50 transient steps, $1 \cdot 10^{-6}$ s (PISO)
Mesh size	$7 \cdot 10^6$ elements

TRANSFER FROM GAS TO LIQUID

Liquids and gases differ most dominantly in their compressibility, density and viscosity. Compressibility and density influence both, the ideal and the real mass flow rate. The viscosity only influences the real mass flow rate. The influence of compressibility, viscosity and density on the ideal and real mass flow rate will be discussed. Based on analytical and numerical investigations approaches to quantify those effects are presented.

Compressibility

The results for the ideal mass flow rate depicted in Figure 3 are gained from equations 2, 3 and 5. They are plotted for different static pressures upstream of the orifice p_{1s} , but otherwise constant boundary conditions, over the pressure ratio. The ideal mass flow rate rises with increasing pressure ratio Π for all cases as expected. The pressure p_1 determines the fluid density. Consequently the ideal mass flow rate increases with increasing p_{1s} regardless of the compressibility. It can be seen that the ideal mass flow rate in the incompressible case (equation 5) is always higher than in the compressible case for the same p_1 . This leads to a lower discharge coefficient in the incompressible case.

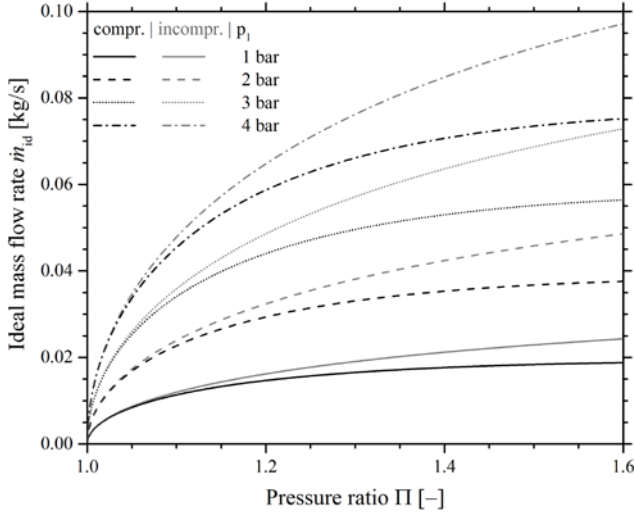


Figure 3: Ideal mass flow rate calculated for a compressible and incompressible flow for different inlet pressures p_1 .

The different densities playing a role in equations 3 and 5 cause this difference. In the compressible case the fluid density downstream of the orifice is applied which is lower than upstream due to the pressure drop. The density decrease is determined by

$$\frac{\rho_1 - \rho_2}{\rho_1} = 1 - \frac{1}{\Pi} \quad (9)$$

The ideal velocity in the orifice is higher in the compressible case than in the incompressible case. This fact originates from the approach for equation 3, which is based on the assumption that an isentropic expansion takes place.

The real mass flow rate through an orifice as described in the previous section is determined numerically, once with an incompressible and once with a compressible fluid model. In Figure 4 the results are plotted over the pressure ratio Π for the same inlet pressure p_1 . The real and ideal mass flow rates for the incompressible case are higher than for the compressible case. Moreover, a stronger deviation between ideal mass flow rates for the incompressible and compressible case is apparent, especially for higher pressure ratios. Regarding the results, it can be concluded that the c_d -values are lower in the incompressible cases.

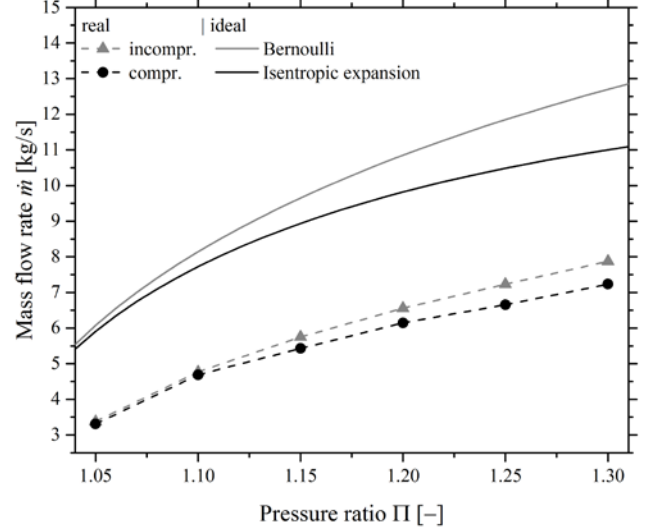


Figure 4: Ideal and real mass flow rate calculated for a compressible and incompressible flow. $p_1 = 1 \cdot 10^5$ Pa

Density

An incompressible fluid with a density ρ_χ , which is χ times higher than the density of air in the reference case ρ_{ref} is considered. The same boundary conditions are applied and all other fluid properties are constant. It is difficult to estimate how the discharge behaviour will change since the density can be eliminated from the c_d -value, leaving only the velocities. The following discussion is based on the assumption of incompressible fluids.

The change of ideal velocity in the orifice is represented by the factor ε which is inversely proportional to the density ratio $\chi = \rho_\chi / \rho_{ref}$ for constant boundary conditions Δp and $v_{1,rel}$. This is based on Newton's first law, as a constant pressure force cannot accelerate a higher mass to the same velocity.

$$\varepsilon^2 = \left(\frac{c_{id,\rho\chi}}{c_{id,\rho ref}} \right)^2 = \frac{2 \Delta p}{2 \Delta p + \rho_{ref} v_{1,rel}^2} \frac{1}{\chi} + \frac{v_{1,rel}^2}{\frac{2}{\rho_{ref}} \Delta p + v_{1,rel}^2} \quad (10)$$

Depending on the boundary conditions ε ranges between 0 and 1 for $\chi > 1$. Increasing the pressure difference causes lower values of ε , which means the influence of density on the ideal velocity in the orifice increases. Increasing the inflow velocity $v_{1,rel}$ results in a higher ε and therefore a higher influence of the density on the ideal velocity $c_{id,rel}$.

The change in ideal mass flow rate can then be expressed by

$$\frac{\dot{m}_{id,\rho\chi}}{\dot{m}_{id,\rho ref}} = \chi \varepsilon = \frac{2 \Delta p + v_{1,rel}^2 \rho_{ref} \chi}{2 \Delta p + v_{1,rel}^2 \rho_{ref}} \quad (11)$$

With the density ratio $\chi = 1$, the ratio in equation 11 is one. Increasing the density ratio causes the ratio of the ideal mass flow rates in equation 11 to rise. Hence, the ideal mass flow rate is always higher for a case with a higher fluid

density, if all other conditions remain the same. Increasing the pressure difference and decreasing the incoming velocity reduces the influence of the density ratio χ on the change of the ideal mass flow rate. This means that the ratio of the ideal mass flow rates from equation 11 is smaller for cases with a higher pressure difference or lower incoming velocity.

In Figure 5 the real velocity in the orifice $c_{re,rel}$, averaged over the orifice area, and the ideal velocity in the orifice $c_{id,rel}$ are plotted over the density ratio χ for two different pressure differences. The ideal velocity in the orifice $c_{id,rel}$ decreases with increasing density ratio. The results from the numerical simulations show that the real velocities in the orifice are always lower than the ideal velocities. Increasing the density of the fluid, while all other parameters remain constant, leads to a decrease of the real velocity $c_{re,rel}$ in the orifice. The decrease of the ideal and real velocity is inversely proportional to the density ratio χ . These findings correspond to the statement in equation 9.

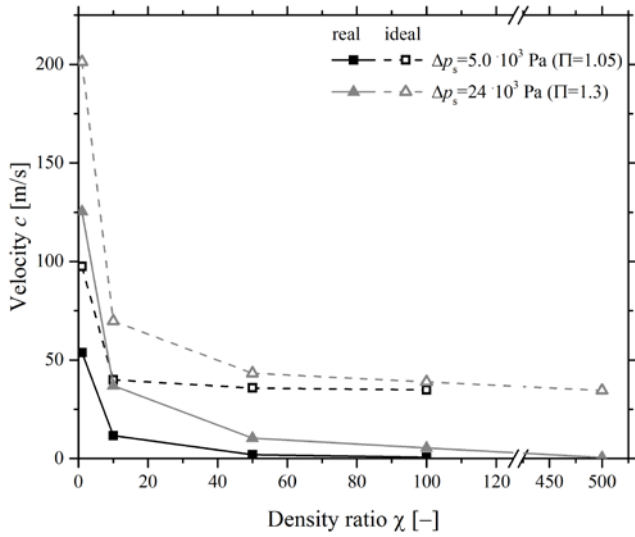


Figure 5: Mean real velocity in the orifice versus the fluid's density

In Figure 6 streamlines projected on the plane parallel to the inflow velocity vector in the absolute reference system are illustrated for the incompressible flow through a rotating orifice. The colour field indicates the fluid velocity. The fluid density for the bottom graph is ten times higher than for the result shown in the top graph. The fluid enters the domain through the inlet on the upper left side and can leave the domain through both outlets on the right side. In both cases a portion of the flow in the outer gap is deflected into the orifice. Within the orifice the flow detaches from the left side and vortices form. Hence the flow is accelerated in the orifice. The flow leaving the orifice impinges on the inner shaft and is eventually deflected radially outwards. The deflection of the flow towards a larger radius occurs earlier for the case with higher density.

The portion of streamlines that enter the orifice from the outer gap is much lower in the case of higher density. Due to a smaller detachment bubble in the case with the lower density, the area the flow passes through is larger. At same

time the velocity of the flow in the orifice is higher in this case with the lower density. It can be estimated from Figure 6 that the decrease of area and flow velocity is lower than the corresponding increase in density. Hence, the real mass flow rate decreases with increasing density.

The observed behaviour is caused by three effects. Firstly, the axis of the orifice is perpendicular to the inflow and outflow. The velocity of the incoming flow is the same for both cases but the density is different. Therefore the flow momentum of the high density fluid is higher. The result is a carry-over effect at the orifice inlet. Consequently, the force necessary to deflect the flow is higher.

Secondly, the centrifugal forces depend directly on the density. They act opposite to the flow direction through the orifice and are thus opposed to the force resulting from the pressure difference across the orifice. This results in a decrease of the real velocity in the orifice, and causes the outwards deflection of the flow to intensify, when the density is increased. For the cases considered here the centrifugal forces amount to a maximum of 28 % of the pressure force. For the scenarios with a higher fluid density the pressure difference needs to be increased to prevent a reverse flow through the orifice.

Thirdly, based on the previous discussion about the ideal velocity a decrease of the real velocity in the orifice is expected with increasing fluid density.

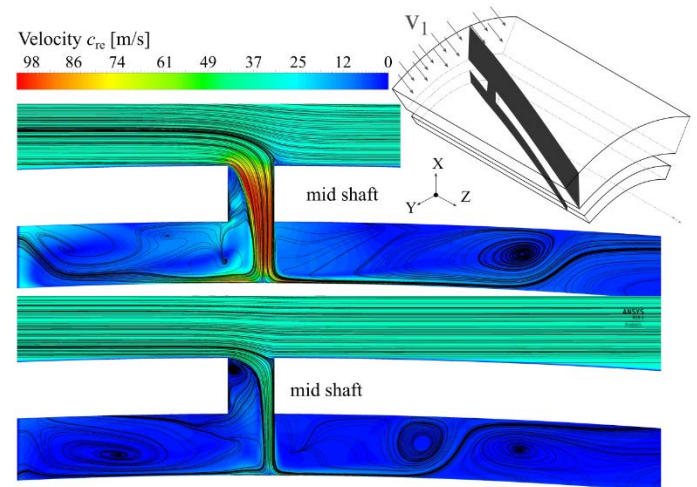


Figure 6: Streamlines of an incompressible flow through a rotating orifice plotted in the plane parallel to the inflow velocity as indicated. Top: Density of air $\rho_{ref} = 1.2 \frac{kg}{m^3}$. Bottom: $\chi = 10$

To investigate the influence of the flow's momentum, simulations with constant momentum of the inlet flow for different fluid densities were conducted. The reference case is run with a density ratio of $\chi = 1$ and an inlet velocity of $v_{ax} = 34$ m/s. Increasing the fluid density and keeping the inlet velocity constant causes the flow's inlet momentum to rise. Consequently, for the cases with a constant inlet momentum the inlet velocity is decreased to match the flow's momentum of the reference case at the inlet. In Table 2 the investigated test cases are listed. For the cases marked by \circ two different

pressure differences of $\Delta p_s = 5 \cdot 10^3$ Pa and $24 \cdot 10^3$ Pa were applied.

For the two cases with the highest density ratio it was necessary to increase the applied pressure difference to ensure that the centrifugal forces acting on the fluid volume in the orifice are significantly lower than the pressure force. For all cases the ratio of centrifugal to pressure forces is smaller than one third.

Table 2: Investigated test cases

χ	Constant inlet velocity	Constant inlet momentum
	$v_{ax} = 34$ m/s	$\dot{m}v = 5.2$ N
Δp_s		
1	○	○
10	○	○
50	○	○
100	○	○
500	$24 \cdot 10^3$ Pa; $50 \cdot 10^3$ Pa	$24 \cdot 10^3$ Pa
1000	$50 \cdot 10^3$ Pa; $100 \cdot 10^3$ Pa	$24 \cdot 10^3$ Pa

In Figure 7 the real velocities in the orifice (a) and the resulting discharge coefficients (b) are plotted over the density ratio χ for two different pressure differences. From the results of the real velocity in Figure 7 (a) it can be seen that the real velocities for the cases with the same density ratios and equal pressure differences are very close. In the case with the same momentum as in the reference case, and hence a lower inlet velocity (dashed line), the real velocity is always higher than in the case with the momentum change and constant inlet velocity (solid line). Considering the ideal case as described in equation 6 it is expected that the velocity in the orifice is lower for the cases with the inlet momentum kept constant, since the inlet velocity is lower. The total relative pressure $p_{t,rel}$ decreases with the square of the inlet velocity. Since the velocity in the orifice $c_{re,rel}$ is higher in the case with the lower inlet velocity, this difference can be attributed to a carry-over effect.

In Figure 7 (b) it can be seen, that increasing the density ratio at a constant pressure difference causes the c_d -value to drop, because the real velocity of the flow in the orifice decreases more strongly than the ideal velocity. Comparing the cases with constant inlet velocity and constant inlet momentum, which differ in their respective inflow velocity, an increase of discharge coefficient c_d can be observed when the inlet velocity is reduced. For the case with $\chi = 10$ the c_d -value reaches almost the reference value if the inlet momentum is constant. For a further increase of the density ratio ($\chi \geq 100$) the c_d -value remains below the reference value. This is due to the increase of the ideal mass flow rate.

As discussed before the influence of the density changes on the discharge coefficient is smaller for the higher pressure difference (compare equation 9).

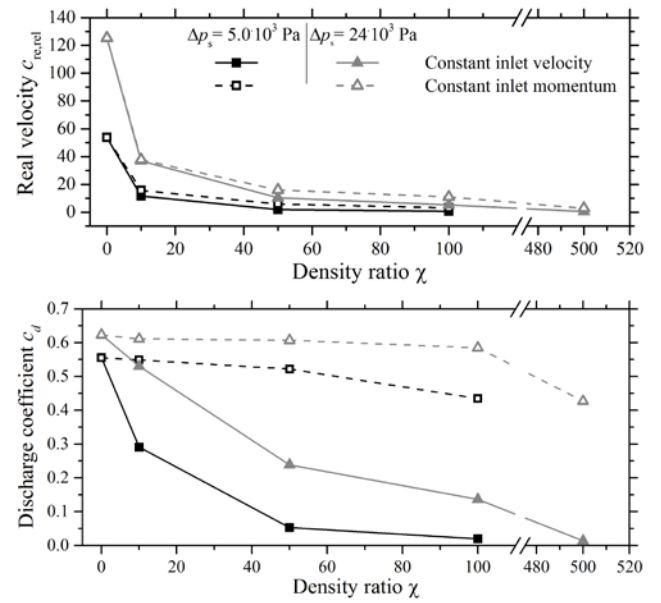


Figure 7 (a) Top: Mean real velocity in the orifice and (b) Bottom: Discharge coefficient over the pressure difference for different densities and inflow momenta.

It can be concluded, that a density increase, while other boundary conditions are constant, causes the ideal and real velocity through the orifice to decrease. The momentum of the flow has an impact on the real flow velocity in the orifice due to a carry-over effect. The inlet velocity determines the total relative pressure and therefore the ideal mass flow rate. The behaviour of the c_d -value with increasing density is more challenging to predict, since ideal and real velocity through the orifice both decrease.

Viscosity

Rising viscosity of the fluid causes the internal fluid friction and friction between fluid and wall, and hence the losses to increase. This leads to lower real mass flow rates, while the boundary conditions remain the same. Therefore the c_d -value decreases with increasing velocity. The Reynolds number, which is the ratio of inertial to viscous forces, is a suitable measure to describe the flow phenomena. Increasing viscosity while all other parameters and boundary conditions remain constant results in a smaller Reynolds number.

In the literature [5] decreasing the Reynolds number is associated with higher discharge coefficients. This discrepancy calls for further investigation. Due to limited computational resources, no simulations were performed and no quantification can be given so far.

COMPARISON WITH LITERATURE

The only available investigation using a liquid flowing through an orifice was conducted by Wilk [12] who found a correlation of the discharge coefficient with the Strouhal number. In Figure 8 the results found in the present study are compared with the correlation by Wilk.

Although, the trends are the same, the results from this study do not fit with Wilk's correlation directly. However a similar correlation was derived for the cases with a constant inlet velocity:

$$c_d = 0.179 \ln\left(\frac{0.54}{S} + 0.83\right) \quad (12)$$

The differences between the correlations are due to the different geometry and inflow conditions, as Wilk investigated axial orifices. The correlation presented in equation (12) includes the carry over effect of the flow over the orifice and the effect of centrifugal forces, which are opposed to the flow direction. While it may be possible to find a correlation for each inflow configuration, this is not the goal of this study. A more suitable parameter to correlate the discharge behaviour that includes the effect of the density, needs to be found.

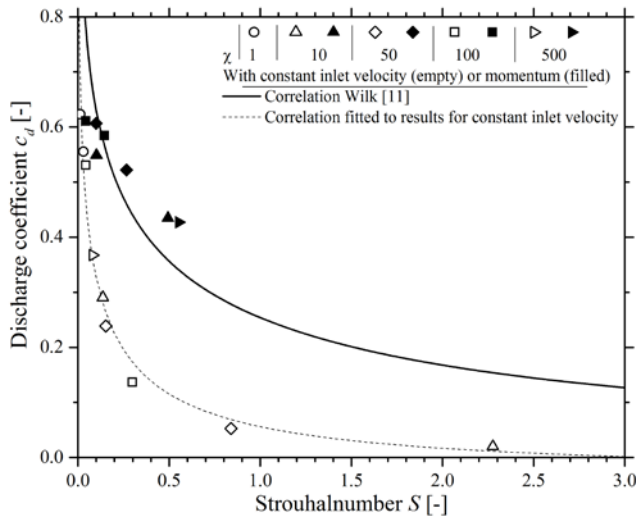


Figure 8: Comparison of the results from this study with Wilk's correlation

In literature the discharge coefficient is often correlated with the incidence angle i or a related ratio (compare Figure 1). In Figure 9 the c_d -values determined in this study are plotted over the incidence angle i . For the cases with a constant inlet velocity (empty symbols) a steady decrease of the discharge behavior with increasing incidence angle can be observed. For the case with a constant inlet momentum no clear trend can be observed, but for all these test cases the incidence angle is smaller than 18° .

For better comparison the data gained from this study is plotted together with data extracted from literature, where a flow through radial orifices in a shaft have been investigated. Results from the work done by Sousek for two different pressure ratios, as well as results presented by Alexiou and Idris are shown.

The results from literature show a decrease of the discharge coefficient with increasing incidence angle, very similar to the results from this study for the case with a constant inlet velocity. The geometry investigated in this study is that used by Sousek. The pressure ratios applied in the

current study correspond to 1.05 and 1.3, which are close to those of Sousek. The higher c_d -values for each dataset were always achieved with the higher pressure ratio.

It can be observed, that the discharge coefficients derived in this study for a constant inlet velocity fit well together with Sousek's results for a pressure ratio of 1.05, even if a higher pressure ratio is applied. This is due to the effects of compressibility or rather lack thereof.

The effect of incompressibility is assessed by comparing the result from the reference case (\circ) for $\Pi = 1.3$ ($i \approx 10$) with the experimental results by Sousek. The c_d -value is lower for the case investigated in the present study. This is in agreement with the expectations derived in the discussion on the effect of incompressibility. The effect of the density change is included in the calculation of the ideal velocity and therefore the incidence angle (compare eq. 6 and Figure 1).

For the cases with a different inlet velocity and constant momentum (squares in Fig. 8) the c_d -values decrease more strongly than results from literature suggest. This can be attributed to the fact that the reduction of the inlet velocity to achieve the same momentum as in the reference case is large. Considering Figure 1 it becomes clear that with a very small relative inlet velocity the incidence angle i is always very small.

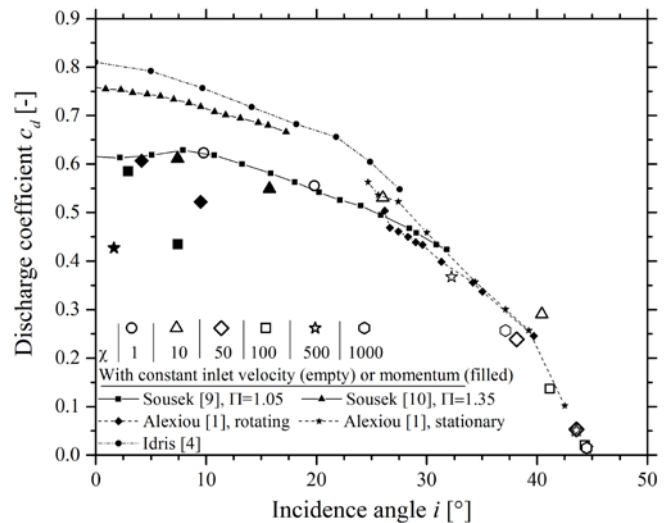


Figure 9: Discharge coefficient over the incidence angle. Comparison with various data.

The calculations with $\chi = 500$ and 1000 were performed with a pressure difference ten times higher than used for lower density ratios of $\Delta p_s = 50 \cdot 10^3$ Pa to overcome the centrifugal forces on the fluid. The excellent agreement with the data from literature demonstrates that the correlation of the discharge coefficient with the incidence angle covers the density influence well.

CONCLUSION

Based on the results of the presented numerical investigation as plotted in Figure 9 and the discussions regarding the effect of incompressibility and density, the following conclusions can be drawn:

- If all boundary conditions are constant, the c_d -value of an incompressible flow through an orifice is lower than that of a compressible one. The reason for this behaviour is the higher ideal mass flow rate of the incompressible flow according to Torricelli's formula.
- With increasing density and all other parameters constant, the ideal and real velocity in the orifice decrease. This is due to a lower acceleration of a higher mass when applying the pressure difference. The ideal velocity is inversely proportional to the density ratio χ and limited by a value depending on the pressure difference and the inlet velocity. It can also be derived that increasing the density leads to a higher inclination angle i .
- The ideal mass flow rate increases with the density for a constant pressure difference. Consequently, the discharge coefficient decreases. The lower real velocity in the orifice of fluids with higher densities reinforces this effect.
- The influence of a density change is lower when a higher pressure difference and a lower incoming velocity is applied. This is explained by the stronger suction effect on the flow through the orifice and the lower momentum of the incident flow. Both effects lead to a higher real velocity and levelling out the consequences of the higher density.

Comparing the findings from this work with the results from literature, e.g. Sousek [10], who investigated the same geometry with an air flow, it can be concluded that the available data for air may be transferred to an incompressible fluid of higher density if an appropriate data correlation is used. Thus, if the dependency of the discharge coefficients from the incidence angle for an air flow through a different orifice geometry is known, the discharge coefficients for a fluid of higher density can be derived. This may include changes of any geometry parameter, such as length, diameter or chamfers. This is especially true if the data is gained for low pressure ratios and therefore in the incompressible regime.

Further research will include experimental results with a real liquid. In this context the influence of the fluid viscosity can be quantified and a comparison with the approaches presented here can be made.

NOMENCLATURE

Latin alphabet

A	area
c	flow velocity in the orifice
c_d	discharge coefficient
i	incidence angle
\dot{m}	mass flow rate
n	rotational speed

Re	Reynolds number
S	Strouhal number
U	orifice velocity
v	velocity
W	velocity in the relative frame of reference

Greek alphabet

β_0	orifice angle of inclination
β_1	inlet relative velocity angle
Δ	difference
ε	ideal velocity ratio
γ	isentropic expansion factor
Π	pressure ratio
ρ	density
χ	density ratio

Indices

1	upstream of orifice
2	downstream of orifice
ax	axial
id	ideal
re	real
ref	reference case
rel	relative reference frame
s	static
t	total

REFERENCES

- [1] Alexiou, A., Hills, N. J., Long, C. A., Turner, A. B., Wong, L.-S., and Millward, J. A. 2000. Discharge coefficients for flow through holes normal to a rotating shaft. *International Journal of Heat and Fluid Flow* 21, 6, 701–709.
- [2] Dittmann, M., Dullenkopf, K., and Wittig, S. Discharge Coefficients of Rotating Short Orifices With Radiused and Chamfered Inlets. In *ASME Turbo Expo 2003, collocated with the 2003 International Joint Power Generation Conference*, 1001–1009. DOI=10.1115/GT2003-38314.
- [3] Dittmann, M., Geis, T., Schramm, V., Kim, S., and Wittig, S. 2002. Discharge Coefficients of a Preswirl System in Secondary Air Systems. *J. Turbomach.* 124, 1, 119.
- [4] Idris, A., Pullen, K., and Barnes, D. 2004. An investigation into the flow within inclined rotating orifices and the influence of incidence angle on the discharge coefficient. *Proceedings of the Institution of Mechanical Engineers, Part A: Journal of Power and Energy* 218, 1, 55–68.
- [5] Idris, A. and Pullen, K. R. 2005. Correlations for the discharge coefficient of rotating orifices based on the incidence angle. *Proceedings of the Institution of Mechanical Engineers, Part A: Journal of Power and Energy* 219, 5, 333–352.

- [6] Idris, A., Pullen, K. R., and Read, R. The Influence of Incidence Angle on the Discharge Coefficient for Rotating Radial Orifices. In *ASME Turbo Expo 2004: Power for Land, Sea, and Air*, 307–320. DOI=10.1115/GT2004-53237.
- [7] Japikse, D. and Baines, N. C. 2007. *Introduction to turbomachinery*. Concepts ETI; Oxford University Press, White River Junction, Vt., Oxford.
- [8] Kader, B. A. 1981. Temperature and concentration profiles in fully turbulent boundary layers. *International Journal of Heat and Mass Transfer* 24, 9, 1541–1544.
- [9] McGreehan, W. F. and Schotsch, M. J. 1988. Flow Characteristics of Long Orifices With Rotation and Corner Radiusing. *J. Turbomach.* 110, 2, 213.
- [10] Sousek, J., Pfitzner, M., and Niehuis, R. Experimental Study of Discharge Coefficients for Radial Orifices in High-Speed Rotating Shafts. In *ASME Turbo Expo 2010: Power for Land, Sea, and Air*, 1051–1060. DOI=10.1115/GT2010-22691.
- [11] Sousek, J., Riedmüller, D., and Pfitzner, M. 2014. Experimental and Numerical Investigation of the Flow Field at Radial Holes in High-Speed Rotating Shafts. *J. Turbomach.* 136, 8, 81009.
- [12] Wilk, A. 2014. Experimental laboratory tests of the pressure drop resulting from the liquid flow through orifices in a rotating disc. *Experimental Thermal and Fluid Science* 54, 297–303.
- [13] Zimmermann, H., Kutz, J., and Fischer, R. Air System Correlations: Part 2 — Rotating Holes and Two Phase Flow. In *ASME 1998 International Gas Turbine and Aeroengine Congress and Exhibition*, V004T09A049. DOI=10.1115/98-GT-207.